

## Post Print

This article is a version after peer-review, with revisions having been made. In terms of appearance only this might not be the same as the published article.

### **Investigation on the sampling size optimisation in gear tooth surface measurement using a CMM**

*International Journal of Advanced Manufacturing Technology, Vol.24 No.7, 2004,  
pp.599-606.*

C.H. Gao, K. Cheng\* and D. Webb

School of Engineering, Leeds Metropolitan University

*Calverley Street, Leeds LS1 3HE, UK*

**Abstract:** Co-ordinate Measuring Machines (CMMs) are widely used in gear manufacturing industry. One of the main issues for contact inspection using a CMM is the sampling technique. In this paper the gear tooth surfaces are expressed by series of parameters and inspection error compensation and initial value optimisation method are presented. The minimum number of measurement points for 3D tooth surfaces are derived. If high precision is required, more points need to be inspected. The sampling size optimisation is obtained from the criterion equation. The surface form deviation and initial values are optimised using the minimum zone method and Genetic Algorithms. A feature based inspection system for spur/helical gears is developed and trials and simulations demonstrated the developed method is very effective and suitable.

**Keywords:** Sampling size optimisation, gear inspection, profile deviation, CMM applications

---

\*Correspondence to: Professor Kai Cheng, School of Engineering, Leeds Metropolitan University, Leeds LS1 3HE, UK.  
Email: k.cheng@lmu.ac.uk

## Notation

$m_n$	normal module
$r$	pitch circle radius
$r_p$	radius of probe
$r_b$	base circle radius
$S_1, S_m, S_o, S_p$	co-ordinate system
$x_0, y_0, z_0$	origin of geometric surface co-ordinate system (o-xyx)
o-xyz	geometric surface co-ordinate system
$O_m-X_mY_mZ_m$	CMM co-ordinate system
$Z_0$	number of gear teeth
$\alpha_1$	pressure angle at point 1
$\alpha_t$	transverse pressure angle
$\beta_b$	base helical angle
$\gamma$	involute function angle
$\Psi$	rotation angle along x axis
$\Phi$	rotation angle along z axis
$\phi$	angle of rotation
$\theta$	initial angle of tooth

$\varphi$  transverse initial angle

## **1. Introduction**

The use of a CMM to inspect gears is becoming increasingly useful in modern gear manufacturing. The actual measurement of gear geometry, using Computer Numerical Control (CNC) machines, is essentially two dimensional even though the gear tooth surfaces are three dimensional. The geometry of the master gear, which is normally the subject of gear inspection, need to be very accurate, and its manufacturing costs are high, especially for small batches.

Generally speaking, the use of small sample sizes is the rule in inspection practice. For example, 3-5 measurement points are used to specify a linear feature, 5-8 points for a plane and 4-8 points for a circle. Adopting such a rule helps to minimise measurement time and to reduce the effect of machine drift (BS 7172) [1].

Hurt [2] has provided simulation-based recommendations for sample sizes to be used for evaluating flatness via least squares. Weckenmann, et al [3] have considered the effect of various sample sizes on least squares estimates of the parameters describing a circular feature. Their studies involved repeated sampling on a given circular part, and they concluded that 10 to 20 points are needed to obtain sufficient precision for

parameter estimates; at least twice the sample size used in practice. Yau and Menq [4] took a more theoretical approach to the choice of sample size. Standard statistical methods were used to develop a hypothesis test on the variance of the residuals that result from a least squares fit, a large variance being indicative of an unacceptable part. A sample size formula was then derived that leads to desired levels of two type errors in their test. This result is important because it shows that the appropriate sample size should depend on both the tolerance specification and the variability of the manufacturing process. The validity of the result depends on having normally distributed deviations, which will not be true in the presence of dominant systematic errors. Strong independence and normality assumptions were made so that basic statistical results apply, but these assumptions may be unrealistic and need to be relaxed.

In their work on 3D gear measurement by a CMM, Lotze and Haertig [5] described how the Involute 97-software package (running under Windows NT/2000) can be used to measure a gear tooth surface. The geometric element, representing the gear flank, is defined by a mathematical parametric equation which contains three parameters- the base radius,  $r_b$ , of the flank origin; the polar angle of the origin and the base helical angle. Gear parameters, such as the lead, profile, pitch and flank form deviation are calculated using this software package based on the measured data. The LK Gear Inspection Software (LKGIS)[6] greatly simplifies the task of inspecting gears. LKGIS provides a logical step-by-step method to help CMM professionals inspect gears quickly. In the work outlined above, probe sampling is not mentioned, even though it may be an essential issue in contact inspection. Many other researchers have also

worked on gear surface inspection, using CMMs to develop analysis algorithms, and to study error compensation. However, more work is required on the use of CMM based gear inspection to optimise sample size inspection.

In this paper, the equations representing the minimum number of measurement points for 2D gear tooth involute curves and 3D tooth surface are derived. These equations can be used to determine the optimal practical sampling size and sample point locations for gear tooth profile/surface inspection. The co-ordinate system transformation error compensation is also investigated, simulation and inspection trials indicated that this optimisation approach is very promising.

## 2. Helical gear tooth surface models

A helical gear tooth surface is generated by an involute curve that performs a screw motion as shown in Fig. 1(a), the equations representing the helical gear tooth surface,

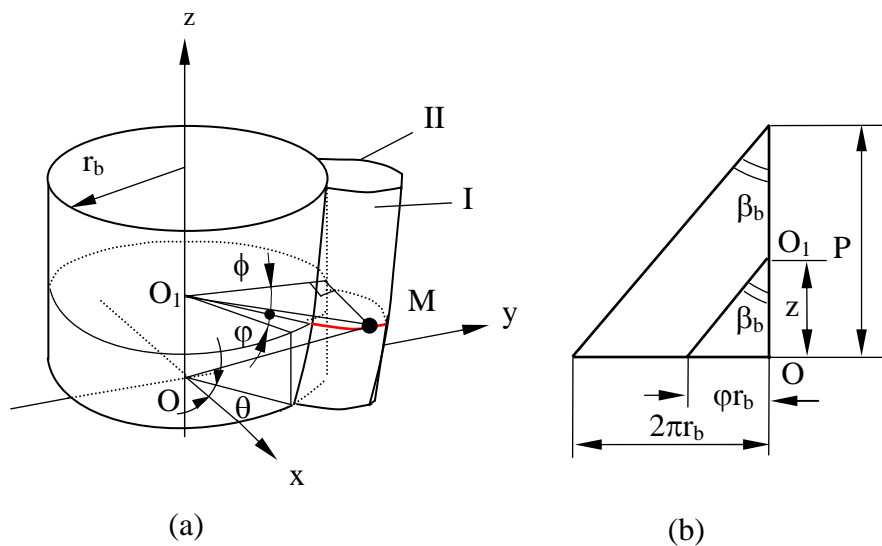


Fig. 1. A tooth surface of a helical gear

their vector equation and surface unit normal can be expressed as[7]

$$\begin{cases} x = r_b [\cos(\theta + \varphi + \phi) + \phi \sin(\theta + \varphi + \phi)] \\ y = \pm r_b [\sin(\theta + \varphi + \phi) - \phi \cos(\theta + \varphi + \phi)] \\ z = \pm \frac{r_b \varphi}{\tan(\beta_b)} \end{cases} \quad (1)$$

$$\begin{aligned} \bar{r} = r_b [\cos(\theta + \varphi + \phi) + \phi \sin(\theta + \varphi + \phi)] \bullet i \pm r_b [\sin(\theta + \varphi + \phi) - \\ \phi \cos(\theta + \varphi + \phi)] \bullet j \pm \frac{r_b \varphi}{\tan(\beta_b)} \bullet k \end{aligned} \quad (2)$$

$$\begin{cases} x = \pm r_b [\cos(\beta_b) \cos(\theta + \varphi + \phi) \pm \sin(\beta_b) \phi \cos(\theta + \varphi + \phi)] \bullet i \pm r_b [\sin(\beta_b) \cos(\theta + \varphi + \phi) \pm \cos(\beta_b) \phi \sin(\theta + \varphi + \phi)] \bullet j \pm \frac{r_b \varphi}{\tan(\beta_b)} \bullet k \\ y = \pm r_b [\sin(\theta + \varphi + \phi) - \phi \cos(\theta + \varphi + \phi)] \\ z = \pm \frac{r_b \varphi}{\tan(\beta_b)} \end{cases} \quad (3)$$

The upper and lower sign in equations (1) - (3) respectively correspond to surface I of the right-hand helical gear (its angles  $\theta$ ,  $\varphi$  and  $\phi$  are measured counterclockwise) and surface II (its angles  $\theta$ ,  $\varphi$  and  $\phi$  are measured clockwise) as illustrated in Fig. 1 (a).  $\theta_j$  is the angle of rotation about the z-axis to bring the j-th tooth to the same position as the first tooth. It is computed as

$$\theta_j = \frac{2\pi(j-1)}{Z_0} + \theta_0 \quad (4)$$

Where  $Z_0$  is the gear tooth number. So, using equations (1) and (4), the equations representing the  $j$ -th tooth surface can be obtained. The equations for a left-hand gear teeth surface can be derived in the same way.

### 3. Measurement error compensation

When a gear is measured on a CMM, it will be set arbitrarily as shown in Fig. 2. There

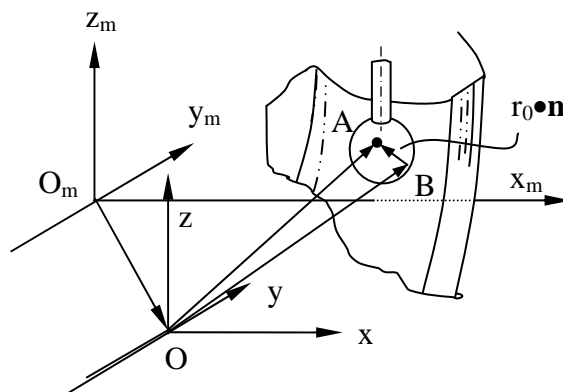


Fig. 2. A tooth surface measurement

are many factors affecting the inspection accuracy during the measurement process. They include the accuracy of the CMM itself, the sampling technique, the co-ordinate system transformation, the probe radius and the algorithm employed, etc. The effects of the co-ordinate system transformation and probe radius will be discussed in this section.

#### 3.1 Co-ordinate system transformation error

The co-ordinate system of the CMM is  $O_m-x_my_mz_m$ , and the  $z_m$  axis is vertical, as shown in Fig. 3. The design co-ordinate system of the gear tooth surface is  $O-xyz$  with its origin locating at  $O(x_0, y_0, z_0)$ . To analyse the inspection results, the inspection datum of the CMM needs to be transformed into the gear geometric design co-ordinate system, as it cannot be assumed that the two coordinate systems correspond. It can be assumed that

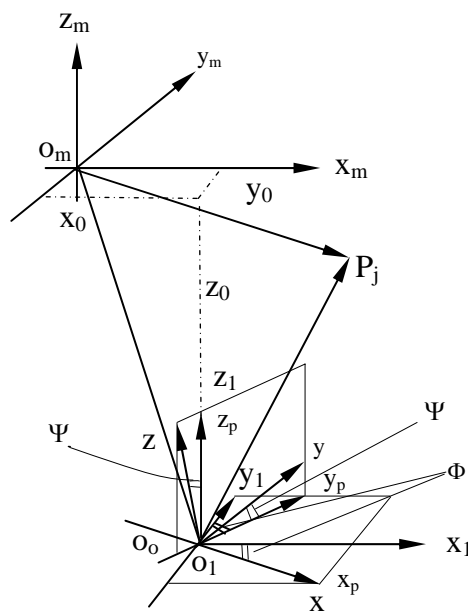


Fig. 3. Co-ordinate systems transformation

there are two rotation angle error factors between the two co-ordinate systems,  $\Psi$  and  $\Phi$ , as shown in Fig. 3. A measurement point  $P(x_m, y_m, z_m)$  on the tooth surface measured using a CMM, has co-ordinates, in the gear design co-ordinate system, which can be expressed as [8,9, 10]



$$\begin{cases} x = x_m \cos \Phi - y_m \sin \Phi - x_0 \cos \Phi - y_0 \sin \Phi \\ y = x_m \cos \Psi \sin \Phi + y_m \cos \Psi \cos \Phi + z_m \sin \Psi - x_0 \cos \Psi \sin \Phi - y_0 \cos \Psi \cos \Phi - z_0 \sin \Psi \\ z = -x_m \sin \Phi \sin \Psi - y_m \sin \Psi \cos \Phi + z_m \cos \Psi + x_m \sin \Phi \sin \Psi + y_m \sin \Psi \cos \Phi - z_0 \cos \Psi \end{cases} \quad (5)$$

Using equation (5), the co-ordinates measured with a CMM can be transformed to the tooth surface design co-ordinate system for analysis.

### 3.2 Probe radius error

When a point is measured on the gear tooth surface, the inspection datum of a CMM is the centre of the probe, as shown in Fig. 2. If the probe tip is of radius  $r_p$ , then

$$\overline{OB} = \overline{OA} - r_p \bullet n \quad (6)$$

$$r_{OB} = r_0 - r_p \bullet n \quad (7)$$

Where,  $\mathbf{n}$  is the unit normal of the helical gear tooth at point B. The inspection datum, in the gear design co-ordinate system, will be

$$\begin{cases} x = x_m \cos \Phi - y_m \sin \Phi - x_0 \cos \Phi - y_0 \sin \Phi - r_p \bullet n_x \\ y = x_m \cos \Psi \sin \Phi + y_m \cos \Psi \cos \Phi + z_m \sin \Psi - x_0 \cos \Psi \sin \Phi - \\ \quad y_0 \cos \Psi \cos \Phi - z_0 \sin \Psi - r_p \bullet n_y \\ z = -x_m \sin \Phi \sin \Psi - y_m \sin \Psi \cos \Phi + z_m \cos \Psi + x_m \sin \Phi \sin \Psi + \\ \quad y_m \sin \Psi \cos \Phi - z_0 \cos \Psi - r_p \bullet n_z \end{cases} \quad (8)$$

To improve the measurement accuracy, the probe radius error can be compensated using equations defined above.

### 3.3 Initial values optimisation

Equation (5) can also be expressed as M ( $M_r$ ,  $M_\theta$ ,  $M_z$ ) in a cylindrical co-ordinate system, as follows

$$\begin{cases} M_r = \sqrt{x^2 + y^2} \\ M_\theta = \arctan\left(\frac{y}{x}\right) \\ M_z = z \end{cases} \quad (9)$$

The point M can also be expressed in the gear co-ordinate system (as shown in Fig. 2.) to cylindrical co-ordinate system as

$$\begin{cases} P_r = \sqrt{P_x^2 + P_y^2} \\ P_\theta = \arctan\left(\frac{P_y}{P_x}\right) \\ P_z = P_z \end{cases} \quad (10)$$

For the same point, the error is the difference between the theoretical value and measured value. That is

$$E = P_\theta - M_\theta = \arctan\left(\frac{P_y}{P_x}\right) - \arctan\left(\frac{y}{x}\right) \quad (11)$$

Using the method of least squares, the co-ordinate transformation errors can be obtained as follows.

$$F = \sum_{j=1}^{z_1} E_j^2 \quad (12)$$

$$\begin{cases} \frac{\partial F}{\partial x_0} = 0, & \frac{\partial F}{\partial y_0} = 0, & \frac{\partial F}{\partial z_0} = 0, & \frac{\partial F}{\partial \Phi} = 0, & \frac{\partial F}{\partial \Psi} = 0 \end{cases} \quad (13)$$

Equation (13) is a non-linear equation and a genetic algorithm can be used to search for the optimal values of  $x_0, y_0, z_0, \Psi$  and  $\Phi$  [11, 12, 13].

#### **4. Sampling size optimisation**

##### **4.1 Minimum number of inspection points for a planar involute curve**

When the initial angle of the involute curve is not equal to zero ( $\theta \neq 0$ ) and the base circle centre is not located at the co-ordinate system origin, as shown in Fig. 4, then

$$\begin{cases} x = x_0 + r_b[\cos(\phi + \theta) + \phi \sin(\phi + \theta)] \\ y = y_0 + r_b[\sin(\phi + \theta) - \phi \cos(\phi + \theta)] \end{cases} \quad (14)$$

In the above equations, parameter  $\phi$  is expressed as

$$\phi = \sqrt{\frac{(x - x_0)^2 + (y - y_0)^2}{r_b^2} - 1} \quad (15)$$

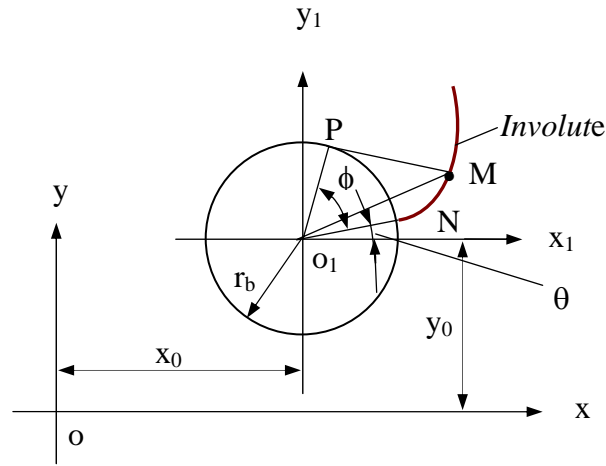


Fig. 4. General planar involute curve

Equations (14) and (15) yield

$$\begin{cases} \phi = \sqrt{\frac{(x - x_0)^2 + (y - y_0)^2}{r_b^2} - 1} \\ (x - x_0) + (y - y_0) = r_b(1 + \phi)(\sin(\phi + \theta)) \end{cases} \quad (16)$$

There are four unknowns ( $r_b$ ,  $x_0$ ,  $y_0$ ,  $\theta$ ) in equation (16). So theoretically, four measurement points  $M_1(x_1, y_1, z_1)$ ,  $M_2(x_2, y_2, z_2)$ ,  $M_3(x_3, y_3, z_3)$ ,  $M_4(x_4, y_4, z_4)$ , are needed in

order to determine their values. Therefore, to evaluate an involute curve feature, one point needs to be measured when the base circle centre locates at the origin and  $\theta=0$  ( see technological report). At least two points need to be measured when the base circle centre locates at the origin and  $\theta \neq 0$ . A minimum of three points need to be measured when base circle centre is arbitrary and  $\theta=0$ . For a general planar involute curve, whose base circle centre is arbitrary and  $\theta \neq 0$ , a minimum of four points need to be measured to determine its geometric features.

#### 4.2 Minimum number of inspection points for a helical gear tooth surface

As the gear design co-ordinate system is not the same as the co-ordinate system for the CMM, the gear tooth surface will be expressed as

$$\begin{cases} x = x_0 + r_b [\cos(\theta + \varphi + \phi) + \phi \sin(\theta + \varphi + \phi)] \\ y = y_0 + r_b [\sin(\theta + \varphi + \phi) - \phi \cos(\theta + \varphi + \phi)] \\ z = z_0 + \frac{r_b \phi}{\tan(\beta_b)} \end{cases} \quad (17)$$

Which yields

$$\left\{ \begin{array}{l} \phi = \sqrt{\frac{(x-x_0)^2 + (y-y_0)^2}{r_b^2} - 1} \\ \varphi = \frac{(z-z_0) \tan(\beta_b)}{r_b} \\ (x-x_0)\phi + (y-y_0) = r_b(1+\phi^2)[\sin(\phi + \theta + \varphi)] \end{array} \right. \quad (18)$$

Equation (18) is equivalent to

$$f(x_0, y_0, z_0, r_b, \beta_b, \theta) = 0 \quad (19)$$

There are six unknowns ( $x_0, y_0, z_0, r_b, \beta_b$  and  $\theta$ ) in equation (19). So for a general helical gear tooth surface, six points need to be measured to determine its geometric surface features using equation (19), which is non-linear equation and can be solved using Genetic Algorithm. Therefore, a general helical gear tooth surface can be obtained if six distributed points are measured on the tooth surface.

### **4.3 Recommended minimum number of measurement points - mathematical approximation method**

Section 4.2 presents mathematically the minimum number of measurement points needed to determine a helical gear tooth surface. Increasing the total number of measurement points above the minimum is expected to have a statistically beneficial effect. This is particularly important if the error of the measurement is comparable to the machining error. The measurement of too many points may make the process

inefficient and is sometimes unnecessary. Generally however, the greater the number of appropriately distributed measured points the more reliable the assessment is likely to be [1]. To conduct a feasible high precision industrial inspection using a contact probe method sampling size optimisation is necessary.

Supposing  $(x_{m1}, y_{m1}, z_{m1}), (x_{m2}, y_{m2}, z_{m2}), (x_{m3}, y_{m3}, z_{m3}), (x_{mn}, y_{mn}, z_{mn})$  are co-ordinates on a tooth surface measured using a CMM, the datum can be transformed to the geometric surface co-ordinate system using equation (8). The difference between the inspected co-ordinate of a point  $i$  and its theoretical value is presented as

$$\nabla_i = f_{y_i} - y_i \quad (20)$$

Where

$$f_{y_i} = y_0 - \phi(x_i - x_0) + r_b(1 + \phi^2) \sin(\theta + \phi) \quad (21)$$

Then

$$\nabla_i = y_0 - \phi(x_i - x_0) + r_b(1 + \phi^2) \sin(\theta + \phi) - y_i \quad (22)$$

So for the whole measured surface, the difference is

$$(23)$$

$$E = \sum_{i=1}^n \nabla_i = \sum_{i=1}^n (f_{y_i} - y_i)^2$$

To minimise this difference,

$$\frac{\partial E}{\partial \theta} = 0 \quad (24)$$

Genetic algorithm is used for searching the optimal solution of the non-linear equations expressed by (24) [14, 15]. The deviation of the tooth surface is given by:

$$F_i = r_b \nabla \theta_i \cos(\beta_b) \quad (25)$$

$$\nabla \theta_i = \theta_{i_{\max}} - \theta_{i_{\min}} \quad (26)$$

Theoretically, as the number of measurement points,  $n$ , is increased, the tooth surface form deviation  $F$  will approach the real practical surface deviation. That is:

$$\Delta F = F_i - F_{i-1} \rightarrow 0 \quad \text{when } n \rightarrow \infty \quad i = 1, 2, 3, \dots, n \quad (27)$$

The deviation  $F_i$  will be the surface deviation when

$$\nabla F_i < \xi \quad (28)$$



Where  $i$  is the recommended minimum number of measurement points.  $\xi$  is the

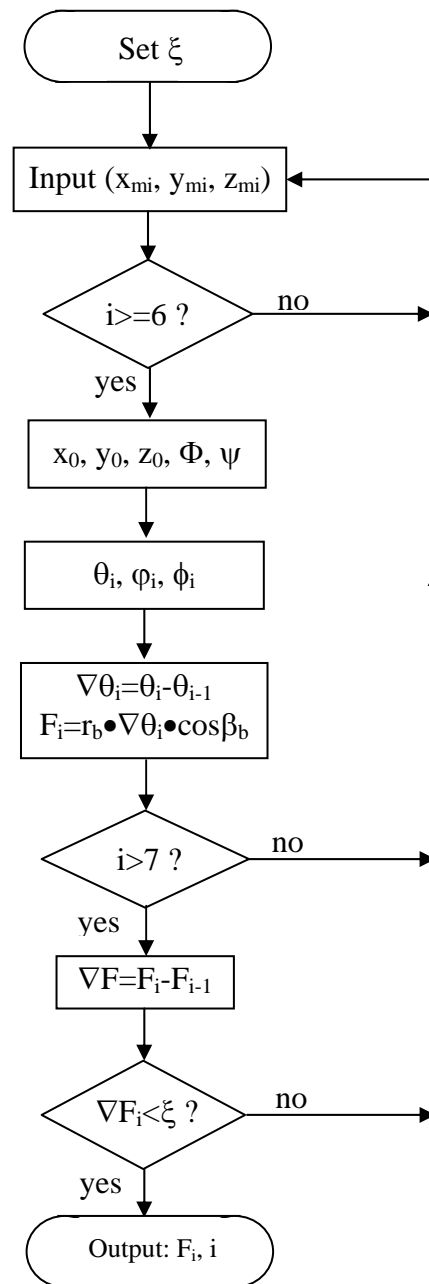


Fig. 5. Computing algorithm for surface form deviation and optimum sampling size

predefined surface inspection accuracy, which is dependent on its precision grade and manufacturing method of the gear. The computing algorithm for the surface deviation and optimum sampling size is shown as Fig. 5. A gear, with  $m_n=4$ ,  $Z_0 =12$  and

$\beta_b=17.45^\circ$ , is used to simulate the inspection algorithm. Both the tooth surface form deviation and sampling location is randomly generated. The initial tooth angle is set to  $0.1^\circ$ , and the error range as  $0.01^\circ$ . The initial value of  $\xi$  is set to 0.0005 mm. The results of the simulation are shown in Fig. 8. They show that as the sampling size increases, the tooth surface deviation will approach its practical form deviation of  $F_i$  (0.0177 mm in this simulation). As the sampling size increases, the difference between  $F_i$  and  $F_{i-1}$  decreases.

## **5. Sampling location**

Its aim is to develop strategies for the distribution of data points to cover the range of characteristic shapes expected from the results of machine and part error analysis, while using the minimum measurement time. Sampling theory is well developed in electrical engineering [16] and several statisticians have written textbooks for the more general cases [17]. The contact inspection and non-contact inspection are normally used in engineering metrology. Contact inspection is popular in industry now, especially in high precision inspection. The issue of where to optimally inspect the surface of the manufactured product is still very important and worth pursuing.

Generally speaking, the distribution of measured data points should normally aim for a uniform coverage of the work-piece. This will help to ensure that the points provide a genuine representation of the geometric features. For gear tooth surface sampling, the points can be placed on parallel section of the tooth surface. The section number  $n_c$  is determined by the gear tooth width. For each of  $n_c$ , approximately uniformly spaced

**Table 1. Distribution results of points on gear sampling**

	ZG320	ZSH1550	ZSH2550	ZSH320	ZSH412
Teeth number	20	50	50	20	12
Module	3	1.5	2.5	3	4
Tooth width	20	15	20	36	48
Sampling size	18	15	18	16	16
$n_c$	3	3	3	4	4
$n_p$	6	5	6	4	4

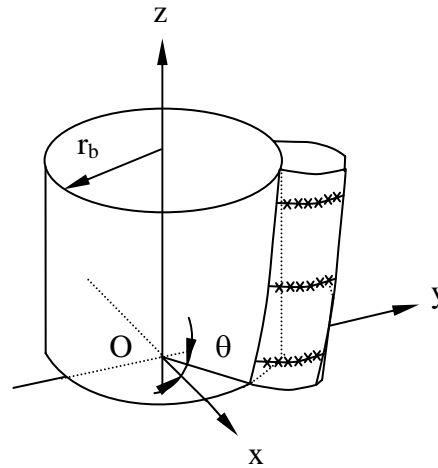


**Fig. 6. Sampling location on measured tooth surface**

planes along the tooth surface, the sampling number in each section  $n_p$  should approximately uniformly be spaced at the intersection of the plane and tooth surface, as shown as Fig 6. The distribution results of sampling points on gear tooth surface are shown as Table 1.

## **6. A case study**

A bench type CMM (Micromasure™ III Brown & Sharpe) was used in the inspection trials as shown in Fig. 7(a). The radius of the spherical probe used was 0.995 mm. Fig. 7(b) shows a screen copy of the gear inspection software system developed by the



Fig. 7. Measurement system and Interface of the developed inspection system

**Table 2. Parameters of the gears used in the trials**  
(a) (b)

Gears	ZG320	ZSH1550	ZSH2550	ZSH320	ZSH412
Number of teeth	20	50	50	20	12
Module (mm)	3	1.5	2.5	3	4
Helical angle (°)	Spur gear	17.45	17.45	17.45	17.45
Pressure angle (°)	20	20	20	20	20
Material	White	White	White	White	Steel
	Delrin	Delrin	Delrin	Delrin	214M15
Direction of spiral	Spur gear	Right hand	Right hand	Right hand	Right hand
Tooth width (mm)	20	15	20	36	48

authors. The system was developed with MATLAB and C++ programming. The parameters of the gears inspected are listed in Table 2.

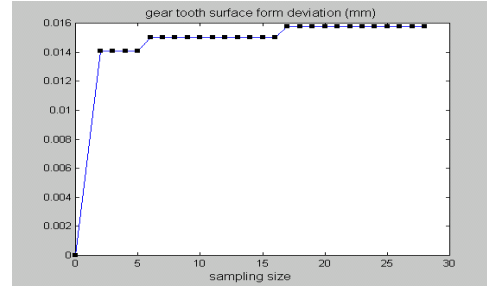
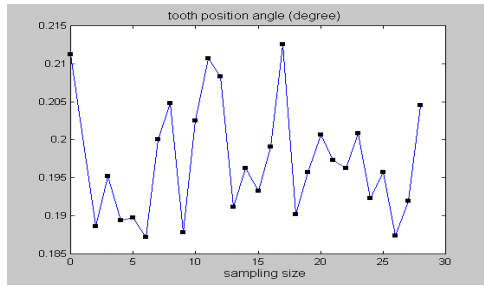
The measured data points should normally be distributed uniformly over the measured surface. This will help to ensure that the points provide a genuine representation of the geometry. The location of the sampling points on the gear tooth surface as recommended by British Standard BS 7172 is shown in Fig. 6. The measured surface data were saved as text files that then analysed by the evaluation module of the system. The initial set up values of  $x_0$ ,  $y_0$ ,  $z_0$ ,  $\psi$  and  $\Phi$  were obtained by a least squares method or the minimum zone method depending on equations (25) and (26). The 3D tooth surfaces were determined from discrete measurement data for the gear tooth. For the  $p^{\text{th}}$  tooth of a gear measured, the gear surface profile deviation will be

$$\nabla F_p = \min\{\max(\nabla f_{p_j}) - \min\{\nabla f_{p_j}\}\} = r \cdot \nabla \theta_p \cdot \cos \beta_b \quad (j = 1, 2, 3, \dots, N) \quad (29)$$

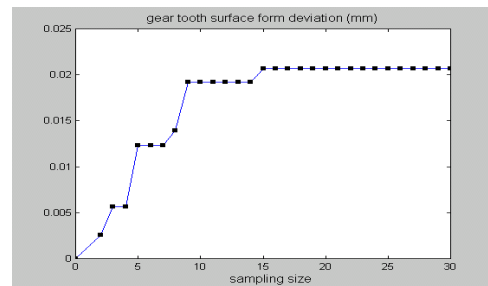
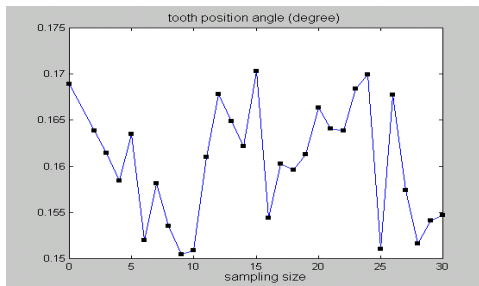
Where,  $r$  is the pitch circle radius. For many scattered measurement points on the gear tooth surface, the surface deviation can be obtained from the optimisation and evaluation algorithms. The results of the inspection trials on four different helical gears are shown in Fig. 8. From the results, it is found that

- 1) The trial results are almost the same as those of the simulations.
- 2) The gear tooth surface profiles were grade 8, as inspected by the gear manufacturer.

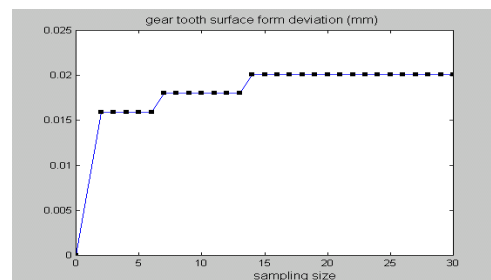
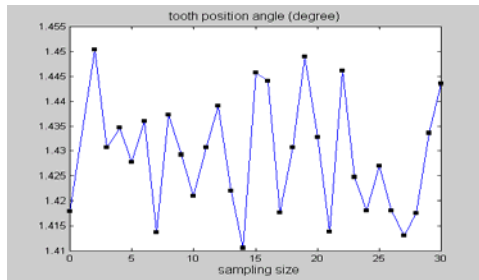
3) The optimal sampling size was around 15.



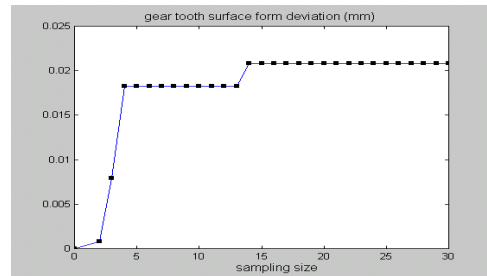
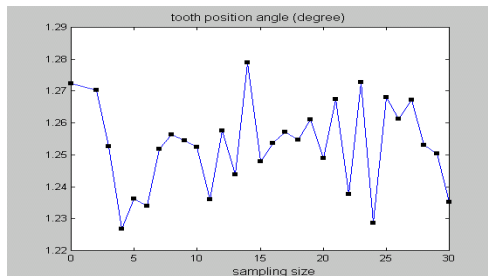
(a) ZSH1550,  $F_1=0.0158$  mm



(b) ZSH2550,  $F_1=0.0208$  mm



(c) ZSH320,  $F_1=0.0199$ mm



(d) ZSH412,  $F_1=0.0219$ mm

Fig. 8. Tooth surface profile deviations of four gears as inspected

Table 3 summarises the tooth form deviations of the four gears inspected. The results illustrate that the deviations are slightly larger (1.04-1.13 times) when using the least square method than for those using the minimum zone method. Therefore, the minimum zone method is recommended for better quality control of the tooth surface profiles.

**Table 3. The tooth surface total profile deviation of the gears**

<b>Gear code</b>	<b><math>f_{LS}(um)</math></b>	<b><math>f_{MZ}(um)</math></b>	<b><math>f_{LS}/f_{MZ}</math></b>	<b>Note</b>
ZG320	19.2	17.1	1.12	Spur gear
ZSH1550	16.9	15.8	1.07	Helical gear
ZSH2550	21.6	20.8	1.04	Helical gear
ZSH320	22.3	19.9	1.12	Helical gear
ZSH412	24.8	21.9	1.13	Helical gear

## 7. Conclusions

In this paper, a sampling optimisation method is proposed for gear tooth surface inspection using a CMM. The minimum number of measurement points required to specify a 2D involute curve is

- 1) One point, when the base circle centre locates at the co-ordinate system origin and  $\theta=0$ .
- 2) Two points, when the base circle centre is at the co-ordinate system origin and  $\theta \neq 0$ .
- 3) Three points, if the base circle is not at the co-ordinate system origin and  $\theta=0$ .

- 4) Four points, if the base circle centre locates at the co-ordinates system origin and  $\theta \neq 0$ .

For a general 3D tooth surface, the minimum number of inspection points should be at least six. For a higher precision requirement, more than six points will be needed. The sampling size optimisation will be obtained based on the criterion expressed in equation (29) in association with the developed method, design tolerance and machining precision. The simulation and inspection trial results have demonstrated that the present approach is very effective and quite suitable for spur and helical gear surface inspection, especially in the shop-floor production environment.

### **Acknowledgements**

The authors would like to thank HPC Gears Ltd. for their technical assistance and gear samples provided.

### **References**

1. Assessment of position, size and departure from nominal form of geometric features, British Standards Institution, BS 7172.
2. J.J. Hurt, A comparison of several plane fit algorithms, *Annals of the CIRP*, 29, pp.381-384, 1980.
3. A. Weckenmann, M. Heinrichowski and H.J. Mordhorst, Design of gauges and multipoint measuring system using co-ordinate measuring machine data and computer simulation, *Precision Engineering*, 13, pp.203-207, 1991.



4. H. Yau and C. Menq, An automated dimensional inspection environment for manufactured parts using co-ordinate measuring machines, *International Journal of Production and Research*, 30 (7), pp.1517-1536, 1992.
5. W. Lotze & F. Haertig, 3D gear measurement by CMM, *Proceedings of Laser Metrology and Machine Performance V*, Birmingham, UK. pp.333-344, 2001.
6. LK gear inspection software, <http://www.lk-cmm.com/gear.html>.
7. K. Cheng, C.H. Gao and D.K. Harrison, 3D surface profile deviation evaluation based on CMM measured data , Proceedings of the 16th International Conference on Computer Aided Production Engineering , Edinburgh, UK, pp.503-510, 7-9 August 2000.
8. C.H. Gao, K. Cheng and D. Webb, An investigation to surface features inspection on complex shaped components , in 'CD-ROM Proceedings of the IFIP Conference on Feature Modeling and Advanced Design-For-The-Life-Cycle Systems', Valenciennes, France, 12-14 June 2001.
9. F. Litvin, Gear Geometry and Applied Theory, PTR Prentice Hall, 1994.
10. G. James et al., Modern Engineering Mathematics, second edition, Addison Wesley Longman, 1996.
11. R.L. Pattison and J.D. Andrews, Genetic algorithms in optimal safety system design, *Proceedings of the IMechE*, 213, Part E, pp.187-197, 1999.
12. D.E. Goldberg, Genetic Algorithms in Search, Optimisation, and Machine Learning, Addison Wesley Longman, 1989.
13. J. Huang, An exact minimum zone solution for three dimensional straightness evaluation problems, *Precision Engineering*, 23, pp.204-208, 1999.

14. M. Fukuda and A. Shimokohvbe, Algorithms for form error evaluation-methods of the minimum zone and the least squares, *Proceedings of the International Symposium on Metrology for Quality Control on Production*, Tokyo, Japan, pp.197-202, 1984.
15. Y.L. Xiong, Computer aided measurement of profile error of complex surfaces and curves: theory and algorithm, *International Journal of Machining Tools and Manufacturing*, 30 (3), pp.339-357, 1990.
16. , W.G. Cochran, Sampling techniques, second edition, Hohn Wiley & Sons, Inc., 1953.
17. L.R. Rabiner and B. Gold, Theory and Application of Signal Processing, Prentice Hall, New York, 1975.